Mixed-Valence, Layered, Cation Radical Salts of the Ethane-Bridged Dimeric Tetrathiafulvalene $[(EDT\text{-}TTF{-}CH_2{-})_2{}^{\bullet+}][X^-][THF]_{0.5}$, $X^- = FeCl_4^-$, $GaCl_4^-$

Cécile Mézière,[1a] Marc Fourmigué,*[,1a] Enric Canadell*[,1b] Rodolphe Clérac,[1c] Klaus Bechgaard,[1d] and Pascale Auban-Senzier[1e]

Sciences Moléculaires aux Interfaces, FRE CNRS 2068, 2 rue de la Houssinière, BP32229, 44322 Nantes Cedex 3, France, Institut de Ciència de Materials de Barcelona (CSIC), Campus de la UAB, E-08193 Bellaterra, Spain, Department of Chemistry, Texas A&M University, College Station, Texas 77842-3012, Department of Solid State Physics, Risø National Laboratory, DK-4000 Roskilde, Denmark, and Laboratoire de Physique des Solides associé au CNRS, Université Paris Sud, Bât. 510, 91405 Orsay Cedex, France

Received February 21, 2000. Revised Manuscript Received May 17, 2000

The synthesis and X-ray crystal structure of the ethane-linked dimeric tetrathiafulvalene $[(EDT\text{-}TTF{-}CH_2)_2]$, 1,2-bis(ethylenedithiotetrathiafulvalenyl)ethane (**1**), is reported. It oxidizes reversibly at 0.45 and 0.90 V vs SCE. Electrocrystallization in the presence of $[n\text{-}Bu_4N][FeCl_4]$ or $[n\text{-}Bu_4N][GaCl_4]$ affords isostructural, mixed-valence conducting 1:1 salts $[\mathbf{1}^{\bullet+}][FeCl_4^-][THF]_{0.5}$ and $[\mathbf{1}^{\bullet+}][GaCl_4^-][THF]_{0.5}$ whose X-ray crystal structures are described. The intercalation of the tetrahedral anions within the organic slabs and the resulting sliding of the molecular diads on top of each other give rise to both 1D- and 2D-type HOMO··· HOMO interactions whose origin is correlated with the details of the peculiar overlap patterns obtained with those dimeric tetrathiafulvalenes. The weak paramagnetism observed in the $GaCl_4^-$ salt due to the organic spins of the conducting slabs is hidden in the $FeCl_4^-$ salt by the $S = 5/2$ Fe(III) contribution. The absence of sizable magnetic interactions between the organic and $FeCl_4^-$ sublattices is accompanied by weak antiferromagnetic $FeCl_4^-/FeCl_4^-$ interactions, attributable to a short Cl···Cl interanion distance at 3.419(17) Å.

Introduction

Compared with the association of TTF redox units through nonbonded interactions[2] such as hydrogen bonds[3,4] or halogen−nitrogen interactions,[5,6] the *covalent* linking of two or more TTF redox units is expected to introduce a certain degree of coupling[7]—through space or through bond—between the redox moieties and, as a consequence, between the conducting stacks or slabs in their cation radical salts, bringing about the possibility of a three-dimensional conducting system. Furthermore, in two-band systems with a small degeneracy between the bands, the Fermi level is expected to cut several bands, giving rise to an equal number of Fermi vectors, as observed, for example, in $[TTF][Ni(dmit)_2]_2$.[8] In this case, the possible occurrence of a $2k_F$ CDW transition at one Fermi vector should not destroy the whole Fermi surface.[9] Although numerous dimeric tetrathiafulvalenes have been reported in the last 10 years,[10] few such systems have been engaged in conducting cation radical salts. Of particular note are the cation radical salts of the ethylene-bridged dimethyltetrathiafulvalene **2**, recently described[11,12] to form one-dimensional, dimerized or trimerized stacks.

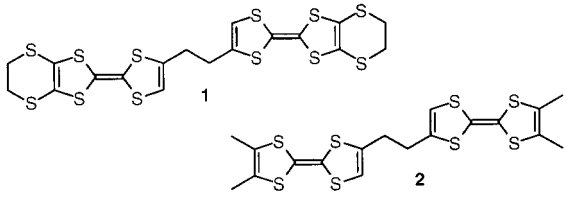

* To whom correspondence should be addressed. E-mail: fourmigue@cnrs-imn.fr.

(1) (a) FRE CNRS 2068. (b) Institut de Ciència de Materials de Barcelona (CSIC). (c) Texas A&M University. (d) Risø National Laboratory. (e) Université Paris Sud.

(2) Desiraju, G. R. *Angew. Chem., Int. Ed. Engl.* **1995**, *34*, 2311.

(3) Dolbecq, A.; Fourmigué, M.; Krebs, F. C.; Batail, P.; Canadell, E.; Clérac, R.; Coulon, C. *Chem. Eur. J.* **1996**, *2*, 1275.

(4) (a) Heuzé, K.; Fourmigué, M.; Batail, P. *Chem. Eur. J.* **1999**, *5*, 2971. (b) Heuzé, K.; Mézière, C.; Fourmigué, M.; Batail, P.; Coulon, C.; Canadell, E. *Chem. Mater.*, in press.

(5) (a) Iyoda, M.; Kuwatani, Y.; Hara, K.; Ogura, E.; Suzuki, H.; Ito, H.; Mori, T. *Chem. Lett.* **1997**, 599. (b) Kuwatani, Y.; Ogura, E.; Nishikawa, H.; Ikemoto, I.; Iyoda, M. *Chem. Lett.* **1997**, 817.

(6) (a) Imakubo, T.; Sawa, H.; Kato, R. *J. Chem. Soc., Chem. Commun.* **1995**, 1667. (b) Batsanov, A. S.; Moore, A. J.; Robertson, N.; Green, A.; Bryce, M. R.; Howard, J. A. K.; Underhill, A. E. *J. Mater. Chem.* **1997**, *7*, 387.

(7) (a) Fourmigué, M.; Huang, Y.-S. *Organometallics* **1993**, *12*, 797. (b) Gerson, F.; Lamprecht, A.; Fourmigué, M. *J. Chem. Soc., Perkin Trans. 2* **1996**, 1409.

(8) (a) Canadell, E.; Rachidi, I. E. I.; Ravy, S.; Pouget, J.-P.; Brossard, L.; Legros, J.-P. *J. Phys.* (*Paris*) **1989**, *50*, 2967. (b) Canadell, E.; Ravy, S.; Pouget, J.-P.; Brossard, L. *Solid State Commun.* **1990**, *75*, 633.

(9) Bechgaard, K.; Lerstrup, K.; Jørgensen, M.; Johannsen, I.; Christensen, J. In *The Physics and Chemistry of Organic Superconductors*; Saito, G., Kagoshima, S., Eds.; Springer Proceedings in Physics 51; Springer-Verlag: Berlin, 1990; p 349.

(10) (a) Otsubo, T.; Aso, Y.; Takimiya, K. *Adv. Mater.* **1996**, *8*, 203. (b) Adam, M.; Müllen, K. *Adv. Mater.* **1994**, *6*, 439.

(11) Rindorf, G.; Thorup, N.; Lerstrup, K.; Bechgaard, K. *Acta Crystallogr.* **1990**, *C46*, 695.

10.1021/cm0001511 CCC: $19.00
Published on Web 07/11/2000

Here, we concentrate on such dimeric systems built on the ethylenedithiotetrathiafulvalene core (EDT-TTF) such as **1**, where the introduction of the outer SCH_2-CH_2S substituents is expected to afford novel conducting materials of higher dimensionality, as demonstrated indeed in its salt[13] with $Au(CN)_2^-$, where interlocked organic slabs adopt a β-type structure. Albeit **2** was observed in its salts as a fully planar molecule adopting the most stable antiperiplanar conformation, possible rotations around the CH_2−(TTF) bonds introduce an additional degree of flexibility in the molecule which can become nonplanar. We describe here the detailed synthesis of **1**, its X-ray crystal structure, and the electrocrystallization experiments with the isosteric $FeCl_4^-$ and $GaCl_4^-$ anions. The conducting and magnetic properties of the two salts will be rationalized through an analysis of their stoichiometry and their peculiar solid-state organization, illustrating the potential of such dimeric molecules toward the elaboration of conducting materials of three-dimensional character.

Results and Discussion

Synthesis and Properties of the Dimeric Donor Molecule. Depending upon the nature of the bridge, two main strategies can be considered for the elaboration of dimeric tetrathiafulvalenes with a single linkage: (i) the association of preformed TTF moieties around the desired spacer or (ii) the formation of the TTF moieties on a difunctional intermediate incorporating the spacer. The first strategy has been mainly used, with monatomic bridges such as S,[14] Se,[14] Te,[15] PPh,[7,16] $SiMe_2$,[7] Hg,[7] or C═O,[17] or diatomic bridges such as vinylene,[18] acetylene,[18] Te−Te,[19,20] or S−S.[21] The second strategy, described for the preparation[22] of **2**, was used here for **1** and implies the formation of the central double bonds of the two TTF moieties in the last step through a Horner−Emmons coupling reaction involving 1,3-dithiole-2-phosphonate anions as nucleophiles and 1,3-dithiole-2-dialkyliminium salts as electrophiles (Scheme 1). The bis(iminium) salt **4** can be prepared from the 1,6-dichloro- (**3a**) or 1,6-dibromo-2,5-hexanedione (**3b**) and 2 equiv of a carbamate salt, followed by cyclization in concentrated H_2SO_4. The synthesis of 1,6-dichloro-2,5-hexanedione (**3a**) has been reported by several authors from the reaction of succinyl dichloride with diazomethane and further treatment of the intermediate 1,6-bisdiazohexane-2,5-dione with HCl.[23] However, the low yield of the reaction (23% from succinyl dichloride) and the hazardous handling of diazomethane in large quantities prompt us to look for alternative procedures starting directly from 2,5-hexanedione. α-Halogenation of ketones is most easily carried out by treatment of the ketones with chlorine, bromine, or iodide. In the present case, however, two possible reaction sites are present and the preferred halogenation sites are expected to be the most substituted ones, in the 3,4-positions. Indeed bromination of 2,5-hexanedione at 0 °C in MeOH afforded mixtures of 1,6- and 3,4-dibromo-2,5-hexanedione. However, performing the bromination at higher temperatures affords a larger amount of the desired 1,6-dibromo-2,5-hexanedione (**3b**) over the other isomer, easily separated by virtue of its lower solubility. Further reaction with 2 equiv of piperidinium carbamate and cyclization in concentrated H_2SO_4 afforded the bis(iminium) salt **4**. Coupling reaction[24,25] with 2 equiv of the phosphonate ester **5** in the presence of *t*-BuOK at −70 °C in THF afforded **1** in low yield after recrystallization from toluene or THF.

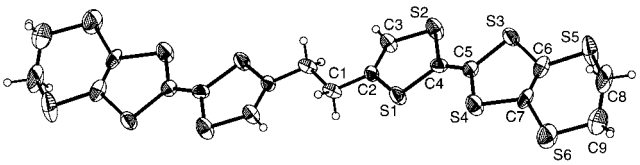

Figure 1. ORTEP view and numbering scheme of the neutral **1** with 50% probability displacement ellipsoids.

Scheme 1

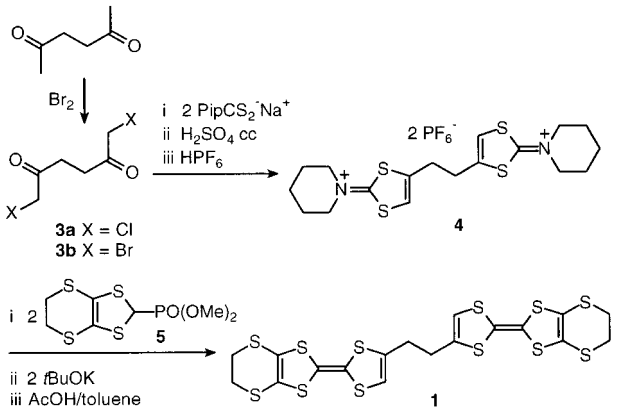

The neutral donor **1** crystallizes in the orthorhombic system, space group *Pnma*. The molecule is located on an inversion center (Figure 1) and exhibits significant deviations from planarity characteristic of such neutral TTF molecules; the outer dithiole ring of the EDT-TTF moiety is indeed folded along the S3- - -S4 axis by 15.9(1)°. The whole molecule adopts the antiperiplanar conformation, a slight torsion around the ethylenic bridge is observed, and the two parallel TTF moieties are not fully coplanar but shifted by 0.28(1) Å, a distortion which confirms the potential flexibility of this molecule. The two EDT-TTF moieties of two neighboring molecules along *b* are related by an inversion center,

(12) Dolbecq, A.; Boubekeur, K.; Batail, P.; Canadell, E.; Auban-Senzier, P.; Coulon, C.; Lerstrup, K.; Bechgaard, K. *J. Mater. Chem.* **1995**, *5*, 1707.
(13) Fourmigué, M.; Mézière, C.; Canadell, E.; Zitoun, D.; Bechgaard, K.; Auban-Senzier, P. *Adv. Mater.* **1999**, *11*, 766.
(14) Bryce, M. R.; Cooke, G.; Dhindsa, A. S.; Ando, D. J.; Hursthouse, M. B.; *Tetrahedron Lett.* **1992**, *33*, 1783.
(15) Wang, C.; Ellern, A.; Becker, J. Y.; Bernstein, J. *Tetrahedron Lett.* **1994**, *35*, 8489.
(16) Fourmigué, M., Batail, P. *Bull. Soc. Chim. Fr.* **1992**, *129*, 29.
(17) Sugimoto, T.; Yamaga, S.; Nakai, M.; Nakatsuji, H.; Yamauchi, J.; Fujita, H.; Fukutome, H.; Ikawa, A.;. Mizouchi, H.; Kai, Y.; Kanehisa, N. *Adv. Mater.* **1993**, *5*, 741.
(18) Otsubo, T.; Kochi, Y.; Bitoh, A.; Ogura, F. *Chem. Lett.* **1994**, 2047.
(19) Becker, J. Y.; Bernstein, J.; Dayan, M.; Shahal, L. *J. Chem. Soc., Chem. Commun.* **1992**, 1048.
(20) Martin, J. D.; Canadell, E.; Becker, J. Y.; Bernstein, J. *Chem. Mater.* **1993**, *5*, 1199.
(21) Leriche, P.; Giffard, M.; Riou, A.; Majani, J.-P.; Cousseau, J.; Jubault, M.; Gorgues, A.; Becher, J. *Tetrahedron Lett.* **1996**, *37*, 5115
(22) Lerstrup, K.; Jørgensen, M.; Johannsen, I.; Bechgaard, K. In *The Physics and Chemistry of Organic Supeconductors*; Saito, G., Kagoshima, S., Eds.; Springer-Verlag: Berlin, 1990; p 383.
(23) (a) Hofman, E. *Chem. Listy* **1951**, *45*, 261; *Chem. Abstr.* **1952**, 7048. (b) Leschke, C.; Altman, J.; Schunack, W. *Synthesis* **1993**, 197. (c) Ippen, J.; Tao-pen, C.; Starker, B.; Schweitzer, D.; Staab, H. A. *Angew. Chem.* **1980**, *92*, 51.

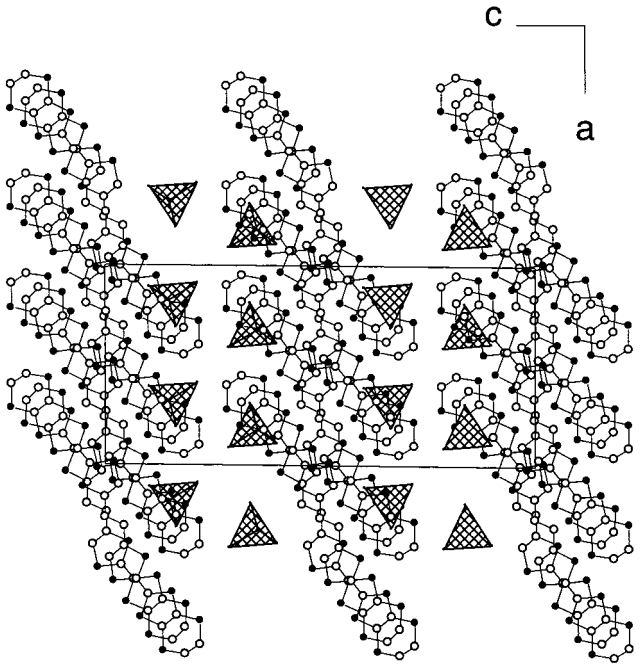

Figure 2. A view of the unit cell of $[\mathbf{1}^{\bullet+}][FeCl_4^-][THF]_{0.5}$. The $FeCl_4^-$ anions are represented as tetrahedrons, and the THF molecules, located on the 2-fold axes, have been omitted for clarity.

giving rise to a diad association with a plane-to-plane distance of 3.54(1) Å, a dimeric motif already encountered in the crystal structure of the neutral EDT-TTF[26] or BEDT-TTF[27] molecules. Electrocrystallization experiments of **1** were conducted in the presence of a variety of anions. Good-quality crystals could be obtained by carefully optimizing the electrocrystallization conditions,[28] and two phases will be described here with the $GaCl_4^-$ and $FeCl_4^-$ anions. Those isosteric tetrahedral anions have been shown to be particularly interesting for providing isostructural materials with contrasted conducting and magnetic properties.[29,30] Of particular interest is the extent of coupling between the conduction electrons of the organic sublattice and the localized spins of the $S = 5/2$ $FeCl_4^-$ anions, while the $GaCl_4^-$ salts provide a pure organic sublattice electronic response.

Mixed-Valence Salts with Monovalent $FeCl_4^-$ and $GaCl_4^-$ Anions. $[\mathbf{1}^{\bullet+}][FeCl_4^-][THF]_{0.5}$ and $[\mathbf{1}^{\bullet+}][GaCl_4^-][THF]_{0.5}$ are isostructural and crystallize in the monoclinic system, space group *C*2/*c*. One organic molecule and one anion are located in general position in the unit cell, and one THF molecule on a 2-fold axis (Figure 2). Because of the 1:1 stoichiometry and the twin character of the donor molecule, the question arises of the extent of delocalization of the positive charge in $\mathbf{1}^{\bullet+}$ between the two EDT-TTF moieties. Bond lengths within the two TTF cores (noted S1−S6 and S7−S9) are given in Table 1 for both salts and compared with those found in the neutral donor molecule and in EDT-TTF itself. The expected lengthening of the central $C_c{=}C_c$ bond and concurrent shortening of the $C_c{-}S$ bonds upon oxidation are observed in both salts although more clearly for the $GaCl_4^-$ salt. A small difference is also observed between the two EDT-TTF moieties, but with no indication of a strong localization of the charge on one of them. Thus, the positive charge in $\mathbf{1}^{\bullet+}$ can be described as shared by both EDT-TTF redox moieties (see later for further discussion), a feature also confirmed by the planarity of the two TTF cores, a signature of such partially oxidized molecules.

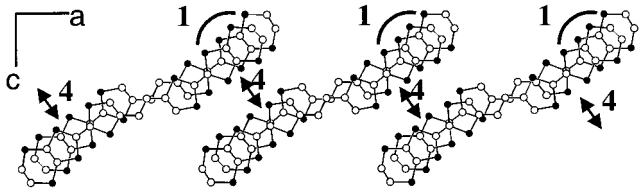

Figure 3. A view of the $(\mathbf{1}^{\bullet+})_2$ diads (interaction 1, bond-over-ring overlap) further interacting through interaction 4, showing the insulating character of the ethylenic bridges.

Table 1. Comparison of Bond Distances within the TTF Core in the Neutral EDT-TTF, 1, and the Salts (Å)

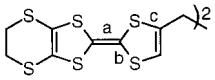

	C−C bond a	C−S bond b	C−S bond c
in neutral EDT-TTF	1.335(4)	1.756(4)	1.758(4)
in neutral **1**	1.335(9)	1.753(8)	1.752(18)
in the $FeCl_4^-$ salt	1.332(9)	1.728(8)	1.746(8)
in the S1−S6 moiety	1.338(9)	1.752(8)	1.752(8)
in the S7−S12 moiety			
in the $GaCl_4^-$ salt	1.381(7)	1.724(6)	1.724(6)
in the S1−S6 moiety	1.380(7)	1.736(5)	1.739(4)
in the S7−S12 moiety			

In the solid state, the donor molecules are associated into inversion-related face-to-face diads with the so-called bond-over-ring configuration (interaction 1 in Figure 3) and a plane-to-plane distance of 3.40 Å, a value well in the expected range for mixed-valence salts. Those diads organize into layers which are interspersed with the tetrahedral anions (Figure 2), an original feature which is not encountered in 2D BEDT-TTF salts where the counteranions are usually localized *between* the organic slabs. Here the tetrahedral anions alternate with the donor diads in the stacking direction *b* and fit in the space delimited by two overlapping molecules. These mixed organic/inorganic slabs are separated from each other by the THF solvent molecules (not shown in Figure 2) located in the interslab space on the 2-fold axes. Of particular note is also a short Cl−Cl distance between two $FeCl_4^-$ anions belonging to two different organic slabs with $Cl(1)\cdots Cl(1)^i$ (i: $-1 - x$, y, $0.5 - z$) at 3.419(17) Å, i.e., shorter than the sum of the van der Waals radii (3.5−3.6 Å). Within the layers, every diad interacts laterally, in the *a*,*c* plane, with two other ones (interaction 4 in Figures 3 and 4). The stacking of those diads in the *b* direction completes the slab, allowing the setting of interactions 2 and 3 (Figure 4).

(24) Jørgensen, M.; Lerstrup, K.; Bechgaard, K. *J. Org. Chem.* **1991**, *56*, 5684.

(25) (a) Fourmigué, M.; Krebs, F. C.; Larsen, J. *Synthesis* **1993**, 509. (b) Krebs, F. C.; Larsen, J.; Boubekeur, K.; Fourmigué, M. *Acta Chem. Scand.* **1993**, *47*, 910. (c) Fourmigué, M.; Johannsen, I.; Boubekeur, K.; Nelson, C.; Batail, P. *J. Am. Chem. Soc.* **1993**, *115*, 3752.

(26) Garreau, B.; De Montauzon, D.; Cassoux, P.; Legros, J.-P.; Fabre, J.-M.; Saoud, K.; Chakroune, S. *New J. Chem.* **1995**, *19*, 161

(27) (a) Kobayashi, H.; Kato, R.; Mori, T.; Ayashi, A.; Saki, Y.; Saito, G.; Inokuchi, H. *Chem. Lett.* **1983**, 759. (b) Kobayashi, H.; Kato, R.; Kobayashi, A.; Mori, T.; Inokuchi, H. *Solid State Commun.* **1986**, *40*, 473.

(28) Batail, P.; Boubekeur, K.; Fourmigué, M.; Gabriel, J.-C. P. *Chem. Mater.* **1998**, *10*, 3005.

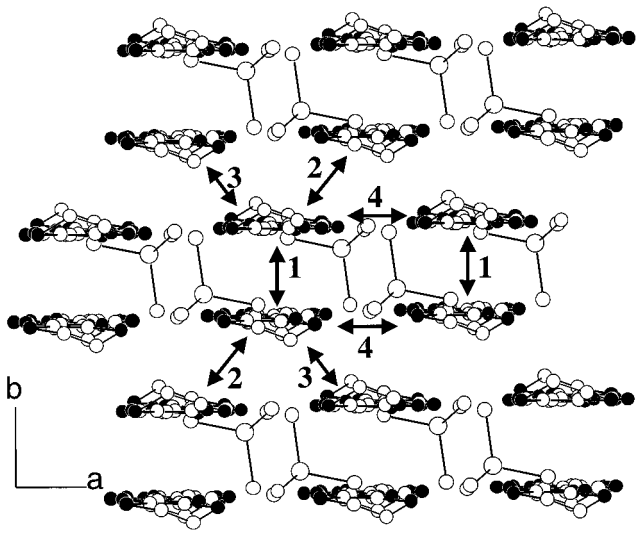

Figure 4. Perspective view of the organic layer of $[\mathbf{1}^{\bullet+}][FeCl_4^-]$-$[THF]_{0.5}$ where the different interactions are defined. Each molecule is viewed approximately along its long axis, and the hydrogen atoms are not shown for simplicity.

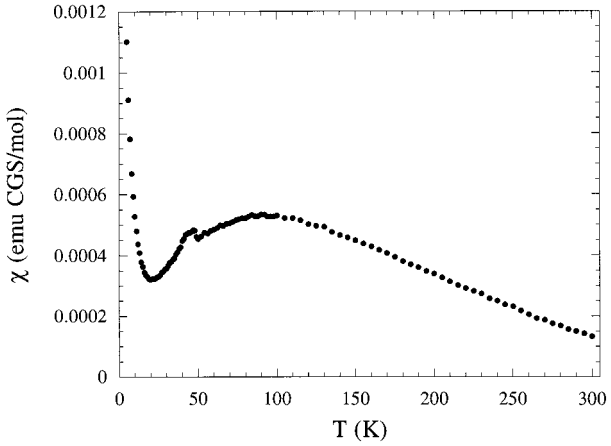

Figure 5. Temperature dependence of the molar SQUID magnetic susceptibility of $[\mathbf{1}^{\bullet+}][GaCl_4^-][THF]_{0.5}$. The features observed at 50 K are attributable to traces of O_2, and the paramagnetism observed at low temperature corresponds to a Curie tail encompassing 1.7% of $S = 1/2$ magnetic defects.

Four-point single-crystal conductivity measurements show a semiconducting behavior with $\sigma_{RT} = 0.025$ S cm^{-1} in both salts and activation energies of 0.078 and 0.081 eV in the $GaCl_4^-$ and $FeCl_4^-$ salts, respectively. Room-temperature ESR measurements performed on a polycrystalline sample of the $GaCl_4^-$ salt show a single signal centered at $g = 2.0062$ with a sharp line width of 15 G, attributable to the organic spins localized on the $\mathbf{1}^{\bullet+}$ moieties. On the other hand, a polycrystalline sample of the $FeCl_4^-$ salt shows a much broader signal, slightly asymmetric, centered at $g = 2.025$ and with a wide line width of ca. 280 G, superposed with a sharp line centered at $g = 2.006$. In the latter, the simultaneous presence of the broad line attributable to the $FeCl_4^-$ anions and the sharp organic line demonstrates the absence of magnetic interactions between the two organic and inorganic sublattices. The magnetic susceptibility temperature dependence of the $GaCl_4^-$ salt (Figure 5) shows a weakly temperature-dependent behavior with a susceptibility maximum around 90 K which reflects the presence of low-dimensional antiferromagnetic interactions between localized electrons such as spin chains or spin ladders (see below). On the other hand, the magnetic susceptibility of the $FeCl_4^-$ salt is dominated by the $S = 5/2$ Fe(III) contribution of the $FeCl_4^-$ anion (Figure 6). In this salt, we expect the magnetic susceptibility to be the sum of the organic (the $\mathbf{1}^{\bullet+}$ cations) and inorganic (the $FeCl_4^-$ anions) sublattice contributions, which were shown to be independent from the ESR results. Furthermore, the close proximity of the $GaCl_4^-$ and $FeCl_4^-$ structures let us infer that the organic sublattice contribution in the $FeCl_4^-$ salt will be comparable to that observed in the $GaCl_4^-$ salt. Accordingly, this organic contribution has been subtracted from the total susceptibility of the $FeCl_4^-$ salt to leave the inorganic sublattice contribution only, χ_i. The temperature evolution of $\chi_i T$ in $[\mathbf{1}^{\bullet+}][FeCl_4^-][THF]_{0.5}$ is shown in Figure 6. Its decrease at the lower temperatures traduces the combined effects of the $FeCl_4^-$ zero-field splitting (ZFS) *and* the eventual presence of $FeCl_4^- - FeCl_4^-$ antiferromagnetic interactions. To distinguish between the two contributions, the tetraethylammonium salt of the $FeCl_4^-$ anion, $[n\text{-}Et_4N^+][FeCl_4^-]$,[31] can be used as a reference compound here for determining the ZFS contribution. Indeed, in this salt, the paramagnetic anions are far from each other; the shortest interanion Cl···Cl distance amounts to 4.233 Å, far above the sum of the van der Waals radii (3.5−3.6 Å). From a fitting procedure developed by Coronado et al.,[32] we deduce a D value of 9.5 K. Taking this value into consideration in the fit of $\chi_i T$ for $[\mathbf{1}^{\bullet+}][FeCl_4^-]$-$[THF]_{0.5}$, we confirm in this salt the presence of a weak antiferromagnetic interaction between $FeCl_4^-$ anions

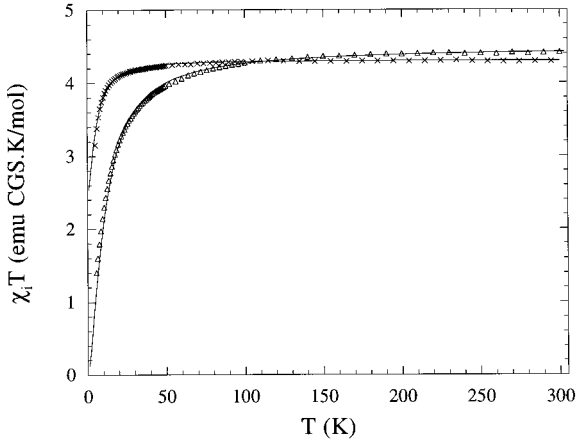

Figure 6. Temperature dependence of $\chi_i T$ for $[n\text{-}Et_4N^+][FeCl_4^-]$ (×) and $[\mathbf{1}^{\bullet+}][FeCl_4^-][THF]_{0.5}$ (△). The solid lines represent the fit to the data with $g = 1.985$ and $D = 9.5$ K in $[n\text{-}Et_4N^+][FeCl_4^-]$ (×) and $g = 2.027$, D = 9.5 K, and $J = -0.8$ K in $[\mathbf{1}^{\bullet+}][FeCl_4^-][THF]_{0.5}$ (△) (see the text).

(29) Kurmoo, M.; Day, P.; Guionneau, P.; Bravic, G.; Chasseau, D.; Ducasse, L.; Allan, M. L.; Marsden, I. D.; Friend, R. H. *Inorg. Chem.* **1996**, *35*, 4719

(30) (a) Kobayashi, H.; Akutsu, H.; Arai, E.; Tanaka, H.; Kobayashi, A. *Phys. Rev.* **1997**, *B56*, R8526. (b) Brossard, L.; Clérac, R.; Coulon, C.; Tokumoto, M.; Ziman, T.; Petrov, D. K.; Laukhin, V. N.; Naughton, M. J.; Audouard, A.; Goze, F.; Kobayashi, A.; Kobayashi, H.; Cassoux, P. *Eur. Phys. J. B* **1998**, *1*, 439. (c) Coronado, E.; Falvello, L. R.; Galan-Mascaros, J. R.; Gimenez-Saiz, C.; Gomez-Garcia, C. J.; Laukhin, V. N.; Perez-Benitez, A.; Rovira, C.; Veciana, J. *Adv. Mater.* **1997**, *9*, 984.

(31) Evans, D. J.; Hills, A.; Hughes, D. L.; Leigh, G. J. *Acta Crystallogr.* **1990**, *C46*, 1818.

(32) BorrasAlmenar, J. J.; Clemente-Juan, J. M.; Coronado, E.; Tsukerblat, B. S. *Inorg. Chem.* **1999**, *38*, 6081.

with $J = -0.8$ K, directly related to the short $FeCl_4^-$/$FeCl_4^-$ distance identified in the crystal structure. The deduced g value for this fit, 2.027, is in very close agreement with the value determined from ESR measurements (see above).

A Complex Interaction Network. It is worth pointing out that the organic sublattice contribution to the susceptibility, unambiguously identified in the $GaCl_4^-$ salt and most probably present in the $FeCl_4^-$ salt, where it is hidden by the $S = 5/2$ $FeCl_4^-$ contribution, can be taken as suggestive of the existence of either spin chains or spins ladders within the donor layers. However, a discussion of the different intermolecular interactions is in order before concluding something about this point. Despite the absence of a metallic state, band structure calculations were performed on the two systems, since they provide important information on the structural and electronic features associated with this class of covalently linked dimeric TTFs. The results of those calculations are nearly identical for both structures, and only conclusions drawn from the $GaCl_4^-$ structure will be described in the following. Since every donor contains two EDT-TTF moieties which are almost uncoupled through the ethylenic bridge, there are two HOMO-type orbitals per donor. For a given molecule, these two orbitals are centered separately on each of the EDT-TTF moieties, at −8.40 and −8.56 eV, the energy difference arising from the slightly different geometries of the two moieties rather than from an internal coupling through the ethylenic bridge. The four different intermolecular interactions identified within a layer are shown in Figure 4. Since there are two HOMO-type orbitals per donor molecule centered on the two EDT-TTF moieties, there are four $\beta_{HOMO-HOMO}$ interaction energies[33] per donor···donor interaction. The largest of the four is 0.396 eV for interaction 1 within the diad, 0.156 and 0.151 eV for interactions 3 and 4 along $-a + b$ and a, respectively, and 0.079 eV for interaction 2 along $a + b$. Clearly though, the diad appears to be the pertinent unit to describe the electronic structure of those slabs. This solves the apparent contradiction raised by the fact that although there is practically no communication between the HOMOs of the two different EDT-TTF moieties, the charge seems to be shared by the two moieties. What really happens is that one electron is housed in the antibonding combination of the two HOMOs of the EDT-TTF moieties involved in interaction 1. Consequently, there is an average of one positive charge per donor molecule, although it should be better described as a +1/2 charge in every EDT-TTF moiety.

The interactions between the neighboring diads lead to the four-band electronic band structure shown in Figure 7 together with the corresponding Fermi surface assuming a metallic filling of the bands. The 1D surface is related to the second highest band in the band structure, which indeed exhibits a very weak dispersion along **Γ** → **M**). It should therefore correspond to an interaction running approximately perpendicularly to $a + b$. On the other hand, the 2D character is attributable to the upper band whose dispersion is important in every direction. To understand the origin of this peculiar behavior, we have calculated the band dispersion for different chains within the organic slab. No dispersion is found in the chains based on diads interacting along a (interactions 1 and 4, Figures 3 and 4), while sizable dispersions are found for chains of molecules linked through interactions 2, 3, and 4 along a, or for diads interacting along $a + b$ (interactions 1 and 2) or along $-a + b$ (interactions 1 and 3). The origin of this absence of dispersion for the diads interacting along a despite the large β value associated with interaction 4 is to be found in the peculiar geometry of this interaction shown in Figure 3. Indeed interaction 4 is fully localized between diads, which are completely isolated from each other by the ethylenic bridges. On the other hand, as shown in Figure 8, interactions 2 and 3 allow a given EDT-TTF moiety to overlap simultaneously with the *two* EDT-TTF moieties of the neighboring molecule; thus, a dispersion along $a + b$ (interaction 2) and $-a + b$ (interaction 3) is found. As noted above, the interactions are stronger along $-a + b$ because of the better geometry and orbital orientation associated with interaction 3. This means that from the point of view of HOMO···HOMO interactions this system should in fact be described as a series of parallel chains of dimers along $-a + b$ interacting moderately along $a + b$, affording a two-dimensional network of

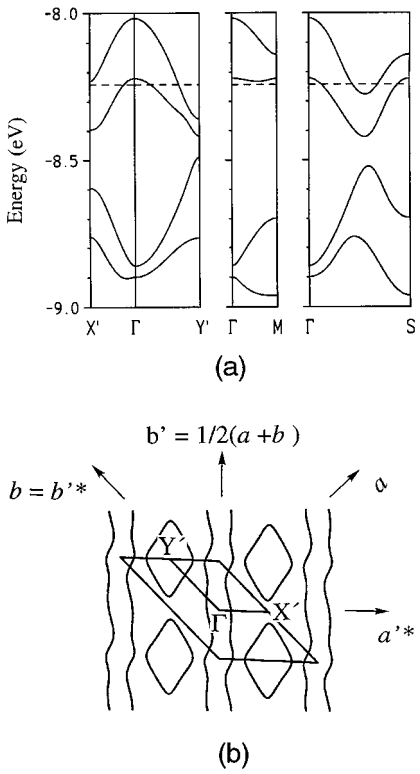

Figure 7. (a) Calculated dispersion relations for the HOMO-type bands of $[\mathbf{1}^{\bullet+}][GaCl_4^-][THF]_{0.5}$ where the dashed line indicates the Fermi level and (b) the associated Fermi surface assuming a metallic filling of the bands. **Γ**, **X′**, **Y′**, **M**, and **S** refer to the wave vectors (0,0), (a'*/2,0), (0,b'*/2), (a'*/2,b′*/2), and (−a'*/2,b'*/2), respectively, where $a' = a$ and $b' = 1/2(a + b)$. Note that the (a',b') cell was chosen since it contains only two molecules, while four molecules should be considered in the original C-centered cell. The calculated band structure and Fermi surface for $[\mathbf{1}^{\bullet+}][FeCl_4^-][THF]_{0.5}$ are almost identical.

(33) Whangbo, M.-H.; Williams, J. M.; Leung, P. C. W.; Beno, M. A.; Emge, T. J.; Wang, H. H. *Inorg. Chem*. **1985**, *24*, 3500. Note that the β interaction energies have the same physical meaning but are not identical to the usual transfer integrals (t) because in extended Hückel calculations overlap is retained.

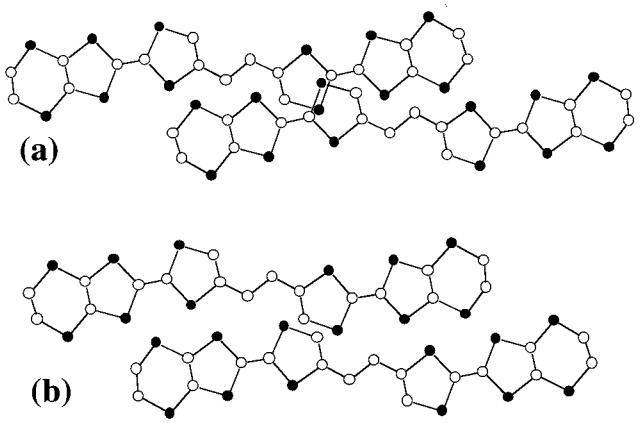

Figure 8. (a) Overlap mode for interaction 2 between two $\mathbf{1}^{\bullet+}$ cation radicals. (b) Overlap mode for interaction 3 between two $\mathbf{1}^{\bullet+}$ cation radicals. Note that one EDT-TTF moiety overlaps with the *two* EDT-TTF moieties of the other molecule, allowing for an EDT-TTF−EDT-TTF intermolecular interaction despite the insulating ethylenic bridge. This is at the origin of the 2D character of the salt.

slightly interacting electrons housed in the EDT dimeric units. The Fermi surface of Figure 7b clearly shows both the presence of chains along $-a + b$ (i.e., the open part approximately perpendicular to $-a + b$), and the coupling between chains (i.e., the closed part), in a way which is clearly reminiscent of the situation in some of the α-phases of BEDT-TTF.[34]

It therefore appears that the $FeCl_4^-$ or $GaCl_4^-$ anions which are included in the organic slab play a crucial role in determining the HOMO···HOMO intermolecular interactions of those salts by displacing the diads relative to each other and thus allowing the interaction geometries 2 and 3, where a EDT-TTF moiety overlaps with two other ones, located above and below. These are the overlap modes which allow the communication among the electrons of the different dimeric units. As a matter of fact, the interaction between electrons in neighboring diads is quite sizable as made clear by the relatively large bandwidths shown in Figure 7a. The dispersion of the partially filled bands is not quite different from that of similar systems exhibiting metallic properties, which suggest quite sizable transfer integrals for the localized electrons of the present salts, something which is in agreement with the small activation energies found in the conductivity measurements. The low activation energy, the chainlike paramagnetism, and the interesting shape of the Fermi surface make the $GaCl_4^-$ salt an attractive candidate for transport property measurements under pressure. It could well be that a metallic state could then be stabilized.

Concluding Remarks

The stabilization of conducting systems exhibiting collective electronic properties requires both the mixed-valence character and the presence of extended overlap interactions of those motifs in the solid. In that respect, a variety of overlap patterns are observed in the structural organization of the bimolecular motifs within one single organic slab in $[\mathbf{1}^{\bullet+}][FeCl_4^-][THF]_{0.5}$ and $[\mathbf{1}^{\bullet+}][GaCl_4^-][THF]_{0.5}$. The fact that some of these overlap modes implicate one EDT-TTF moiety of one donor but both moieties of the other, together with the structural flexibility conferred by the ethane link, leads us to think that it will be possible to prepare 2D metallic systems with linked donors such as **1**. In the ethane-linked dimeric tetrathiafulvalene systems, the extend of interaction between the two EDT-TTF redox moieties through the ethylenic bridge has been shown to be very limited. However, its replacement by a vinylic or acetylenic one might provide a stronger intramolecular interaction pathway and accordingly a stronger inter-slab interaction for the elaboration of conducting materials.

Experimental Section

1,6-Dibromo-2,5-hexanedione (3a). Acetonylacetone (23.5 mL, 0.2 mol) was dissolved in dry MeOH (300 mL) under N_2, and bromine (20.5 mL, 0.4 mol) was added dropwise over 30 min with stirring while the temperature was kept at 25 °C with an ice bath. After being stirred for 30 min, the solution was cooled in an ice bath before 50% H_2SO_4 (50 mL) was added dropwise. The mixture was stirred overnight at room temperature. Water was added slowly to the cold solution (5 °C) to precipitate the white product, which was filtered off, purified by dissolution in CH_2Cl_2 (300 mL), and poured into petroleum ether, where it precipitates (the mother liquors contain mainly 3,4-dibromo-2,5-hexanedione). The bright thin plates obtained were dried under vacuum: yield 19 g (35%); mp 112−113 °C; ^{1}H NMR ($CDCl_3$/TMS) δ = 2.97 (s, 4H, $-CH_2-CO$), 3.95 (s, 4H, $-CH_2-Br$); ^{13}C NMR ($CDCl_3$/TMS) δ = 34.29 (CH_2CO), 34.40 (CH_2Br), 201.04 (C=O); MS (EI) *m/e* (rel intens) 273 (8, M^+), 179 (100), 123 (45), 95 (22). Anal. Calcd for $C_6H_8Br_2O_2$ (Found): C, 26.50 (26.29); H, 2.97 (2.94); Br, 58.77 (58.51); O, 11.77 (11.79).

Preparation of the Bis(iminium) Salt 4. 1,6-Dibromo-2,5-hexanedione (**3a**) (18.6 g, 0.068 mol) was added by small amounts to a solution of piperidinium carbamate (33.7 g, 0.136 mol) in degassed DMF (200 mL) at 0 °C under a nitrogen atmosphere. A white precipitate appeared in the mixture, which was stirred overnight at room temperature. The product was precipitated by being poured into H_2O/ice. The cream solid was filtered, washed abundantly with H_2O, dried in the air, and used in the following step without further purification: yield 29.2 g (99%); mp 143−145 °C; ^{1}H NMR ($CDCl_3$/TMS) δ = 1.70 (m, 12H, $-(CH_2)_3$), 3.00 (s, 4H, $-CH_2-CO$), 3.92 (m, 4H, $-S-CH_2-CO$), 4.23 (s, 8H, $-CH_2-N$); MS (EI) *m/e* (rel intens) 432 (6, M^+), 304 (22), 273 (20), 160 (15), 128 (100).

The crude dicarbamate (29.2 g, 0.067 mol) was slowly added with stirring to concentrated H_2SO_4 (130 mL) at $T < 10$ °C. After being stirred for 2 h at this temperature and 2 h at room temperature, the yellow mixture was poured onto crushed ice containing HPF_6 (60% in water, 19.8 mL, 0.134 mol). The precipitated hexafluorophosphate **4** was washed with copious amounts of water until the washings were neutral, pressed dry on the filter, washed with Et_2O, dissolved in MeCN, and precipitated in Et_2O once again. Recrystallization from ethanol afforded **4** as white crystals: yield 36.2 g (80%); mp 249−252 °C; ^{1}H NMR (DMSO-d_6/TMS) δ = 1.68 (m, 4H, $-CH_2-CH_2-$), 1.79 (m, 8H, $-(CH_2)_3$), 3.14 (s, 4H, $=CH-CH_2$), 3.79 (m, 8H, $-CH_2-N$), 7.42 (S, 2H, $=CH-CH_2$); ^{13}C NMR (DMSO-d_6/TMS) δ = 21.20($NCH_2CH_2CH_2$), 24.45 (NCH_2CH_2), 30.03 (CH_2-CH_2), 55.8 and 56.8 (NCH_2), 119.88 (=*C*H), 137.46 (=*C*−CH_2), 186.82 (*C*=NR_2^+). Anal. Calcd for $C_{18}H_{26}F_{12}N_2P_2S_4$ (Found): C, 31.40 (31.05); H, 3.81 (3.69); F, 33.11 (30.84); N, 4.07 (3.96); P, 9.00 (9.33); S, 18.63 (18.39).

Preparation of 1. The phosphonate ester[35] **5** (13.61 g, 0.045 mol) was dissolved in anhydrous THF (150 mL) and the solution cooled to −78 °C. *t*-BuOK (5.04 g, 0.045 mol) dissolved

(34) Rousseau, R.; Doublet, M.-L.; Canadell, E.; Shibaeva, R. P.; Khasanov, S. S.; Rozenberg, L. P.; Kushch, N. D.; Yagubskii, E. B. *J. Phys. I* **1996**, *6*, 1527.

(35) Moore, A. J.; Bryce, M. R. *Synthesis* **1991**, 26.

Table 2. Crystallographic Data

compound	**1**	[**1**][$GaCl_4$][THF]$_{0.5}$	[**1**][$FeCl_4$][THF]$_{0.5}$
empirical formula	$C_{18}H_{14}S_{12}$	$C_{20}H_{18}Cl_4GaO_{0.5}S_{12}$	$C_{20}H_{18}Cl_4FeO_{0.5}S_{12}$
fw	615.01	862.58	848.71
cryst syst	orthorhombic	monoclinic	monoclinic
space group	Pbca	*C*2/*c*	*C*2/*c*
a/Å	11.649(1)	14.502(1)	14.503(1)
b/Å	9.539(1)	13.915(1)	13.915(1)
c/Å	21.751(3)	31.139(3)	31.148(3)
α/deg	90	90	90
β/deg	90	90.81(1)	90.64(1)
γ/deg	90	90	90
V/Å^3	2417.1(6)	6283(1)	6285(1)
Z	4	8	8
d_{calcd}/Mg m^{-3}	1.690	1.824	1.794
wavelength		Mo Kα, $\lambda = 0.710\ 73$ Å	
temp/K	293(2)	293(2)	293(2)
μ/mm^{-1}	1.092	2.031	1.635
θ range/deg	1.87−25.96	2.0−23.9	2.1−23.8
no. of measd reflns	2947	24 222	17 155
no. of indp reflns	2284	4630	4811
R_{int}	0.1543	0.078	0.1522
abs correction	ψ scan	numerical	numerical
max, min trans	0.893, 0.809	0.925, 0.579	0.972, 0.773
no. of ref params	136	326	326
res in final $\Delta\rho$ map/(e Å^{-3})	0.46, −0.51	0.58, −0.43	0.33, −0.25
largest shift/esd	0.0	0.001	0.014
R^a	0.0546	0.0479	0.0458
Rw^a	0.1133	0.1138	0.0728

[a] $R = \sum|\Delta F|/\Sigma|F_o|$, $Rw = [\sum(\Delta F)^2/\sum wF_o^2]^{1/2}$.

in THF (50 mL) was added dropwise at −78 °C, the solution stirred for 15 min, the bis(imminium) salt **4** (10.33 g, 0.015 mol) added at once, and the suspension stirred for 3 h before being warmed to −10 °C. Et_2O (200 mL) was added to precipitate unreacted salts and the suspension filtered on Celite. The solution was concentrated under vacuum and diluted with toluene (150 mL), and AcOH (∼ 35 mL) was added slowly until the red solution became dark. After being stirred for 1 h, the solution was washed abundantly with water, dried ($MgSO_4$), and filtered through a silica gel column. Recrystallization from THF afforded 1,2-bis(ethylenedithiotetrathiafulvalenyl)ethane (**1**) as bright orange crystals: yield 0.43 g (5%); mp 228−230 °C dec; ^{1}H NMR (DMSO-d_6/TMS) $\delta = 2.66$ (s, 4H, CH_2), 3.39 (s, 8H, S−CH_2), 6.50 (s, 2H, CH); ^{13}C NMR (DMSO-d_6) $\delta = 30.3$, 30.6 (2 CH_2), 102.9, 113.5, 115.6, 119.1, 124.8, 134.7. Anal. Calcd for $C_{18}H_{14}S_{12}$ (Found): C, 35.15 (35.01); H 2.29 (2.21); S 62.56 (61.03).

Electrocrystallization Experiments. Two-compartment cells with platinum electrodes ($l = 2$ cm, $\varnothing = 1$ mm) were used. [**1**$^{\bullet+}$][$FeCl_4^-$][THF]$_{0.5}$: **1** (5 mg) and [*n*-Et_4N^+][$FeCl_4^-$][36] (15 mg) were dissolved in THF (12 mL) and electrocrystallized at constant current (0.5 μA) for 1 week at 40 °C. [**1**$^{\bullet+}$][$GaCl_4^-$][THF]$_{0.5}$: **1** (5 mg) and [*n*-Me_4N^+][$GaCl_4^-$][29] (15 mg) were dissolved in THF (12 mL) and electrocrystallized at constant current (0.3 μA) for 3 weeks at 30 °C.

Data Collection and Structure Determination. Table 2 summarizes the crystallographic details about data collection and structure refinement. Data were collected at room temperature, on an Enraf-Nonius Mach3 diffractometer for **1** and on an Imaging Plate Diffraction System (Stoe-IPDS) for the two salts. Data from the Enraf-Nonius Mach3 diffractometer were processed using the program XCAD4 (K. Harms, University of Marburg). Structures were solved by direct methods using SHELXS-86 and refined by the full-matrix least-squares method on F^2, using SHELXL-93 (G. M. Sheldrick, University of Göttingen, 1993) with anisotropic thermal parameters for all non-hydrogen atoms. The hydrogen atoms were introduced at calculated positions (riding model).

Band Structure Calculations. The tight-binding band structure calculations[37] were of the extended Hückel type.[38] A modified Wolfsberg−Helmholtz formula was used to calculate the nondiagonal $H_{\mu\nu}$ values.[39] Double-ζ orbitals for C and S were used. The exponents and parameters were taken from previous work.[12]

Magnetic Measurements. The ESR spectra were recorded at room temperature on polycrystalline samples with a Bruker ER200D X-band spectrometer operating at 9.3 GHz. Magnetic susceptibility measurements were performed on a Quantum Design MPMS-2 SQUID magnetometer operating in the range 4−300 K at 2000 G with polycrystalline samples of [**1**][$GaCl_4$]-[THF]$_{0.5}$ (17.3 mg) and [**1**][$FeCl_4$][THF]$_{0.5}$ (2.95 mg). Data were corrected for sample holder contribution and Pascal diamagnetism.

Acknowledgment. We thank Dr. L. Bull (Nantes) for the ^{13}C NMR experiments, P. Molinié (Nantes) for the room-temperature ESR measurements, and Dr. J. M. Clemente-Juan and Pr. E. Coronado (Valencia, Spain) for useful discussions. This work was partially supported (E.C.) by DGES-Spain (Project PB96-0859) and Generalitat de Catalunya (Grant 1997 SGR24).

Supporting Information Available: Tables of detailed crystallographic data, positional and thermal parameters, and bond distances and angles, in CIF format. This material is available free of charge via the Internet at http://pubs.acs.org.

CM0001511

(36) Mallah, T.; Hollis, C.; Bott, S.; Day, P.; Kurmoo, M. *Synth. Met.* **1988**, *27A*, 381.

(37) Whangbo, M.-H.; Hoffmann, R. *J. Am. Chem. Soc.* **1978**, *100*, 6093.

(38) Hoffmann, R. *J. Chem. Phys.* **1963**, *39*, 1397

(39) Ammeter, J. H.; Bürgi, H.-B.; Thibeault, J.; Hoffmann, R. *J. Am. Chem. Soc.* **1978**, *100*, 3686.